HQCD: HIC in holographic approach

I. Ya. Aref'eva[1]

,

Moscow, Russia

Steklov Mathematical Institute, Russian Academy of Sciences,
Gubkina str. 8, 119991, Moscow, Russia

Этот доклад посвящен голографической квантовой хромодинамике (ГКХД) с упором на изучение свойств кварк-глюонной плазмы, которые в принципе могут быть получены из экспериментов со столкновениями тяжелых ионов (СТИ). Основной характеристикой является структура фазовой диаграммы, которая делит плоскость (μ, T) на адронную и кварк-глюонную фазы. На этой фазовой диаграмме есть также линия фазового перехода, связанная с нарушением киральной симметрии, а также линия фазового перехода, связанная с кваркионной фазой. Мы представляем голографическую модель, для которой естественно появляется кваркионная фаза. Показано, что линия фазового перехода адронная фаза — кваркионная существенно зависит от анизотропии и, в частности, от магнитного поля.

This contribution is devoted to holographic quantum chromodynamics (HQCD) with a focus on studying the properties of quark-gluon plasma, which can in principle be extracted from experiments with heavy ion collisions (HIC). The main characteristic is the structure of the phase diagram, which divides the (μ, T) plane into an hadronic phase and a quark-gluon phase. In this phase diagram there is also a phase transition line associated with chiral symmetry breaking, as well as a phase transition line associated with the quarkyonic phase. We present a holographic model for which the quarkyonic phase naturally appears. We show that the line of the hadronic phase – quarkyonic phase transition essentially depends on anisotropy and, in particular, on the magnetic field.

PACS: 11.25.Db, 12.38.-t

1. Introduction

In this talk we will discuss the following subjects.

- Physical picture of the formation of quark-gluon plasma (QGP) in collisions of heavy ions.
- Results of applying the holographic approach to the description of heavy ions collisions and properties of the quark-gluon plasma. They include

  – explanation of experimental data:

  in particular, multiplicity of particles production in HIC;

  – prediction of the new effects in anisotropic quark-gluon plasma:

[1]E-mail: arefeva@mi-ras.ru

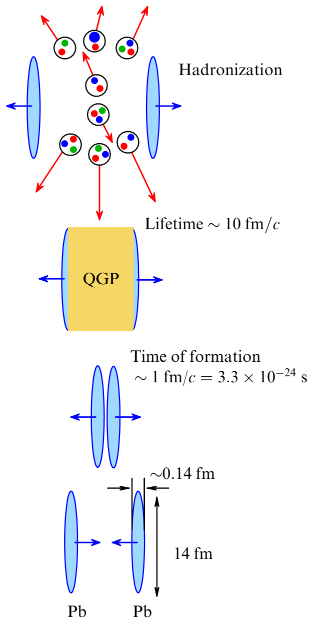

Figure 1: Time evolution of matter created in heavy ion collision, plot from [1].

i) smeared of the confinement/deconfinement phase transition,

ii) dependence of energy losses (jet quenching coefficient) on the anisotropy parameter and chemical potential,

iii) dependence of the emission rate of direct photons on the anisotropy parameter and chemical potential;

- more detailed structure of phase transitions, namely the dependence of the position of the phase transition line on

– quark masses,

– magnetic field magnitudes,

– spatial anizotropy (centrality of HIC)

We will discuss mainly the results on the subjects above obtained in our group at Steklov Mathematical institute and published in references [1–18].

2. Evolution after heavy ion collision

QGP is a state of matter of free quarks, antiquarks and gluons at high temperature. QGP was discovered at RHIC in 2005. QGP behaves (RHIC, LHC) like a strongly interacting fluid (collective effects) [1].

In Fig. 1 the time evolution of matter created in heavy ion collision is presented. It is believed that short after collision of heavy ions the local thermalization takes place. This process is accompanied by a huge production of entropy. The physics is not fully understood. Difficulties arise due to time-dependent non-equilibrium QCD processes. Local thermalization creates an initial condition for hydrodynamic evolution. The hydrodynamic approach is widely used to process the experimental results obtained at the LHC and RHIC.

One can think of QGP as a strongly interacting liquid, and two questions arise regarding this liquid.

1. How was it formed?
2. What properties does it have?

Note that perturbation methods are not applicable to get answers to these questions. Lattice methods also do not work, because we consider the process in real time. In the stationary case the lattice method has problems with the chemical potential. It is possible to use holographic QCD based on gauge/string duality to answer these questions. Note, that holographic method is a phenomenological approach motivated by AdS/CFT duality [19]. Main ingredients of relations between theory in realistic 4-dimensional space-time and theory in deformed AdS are the following (see [1, 20, 21] and refs therein):

- QCD temperature $\Longleftrightarrow$ black hole temperature in a deformed AdS_5,
- thermalization in QCD $\Longleftrightarrow$ formation of black hole in the deformed AdS_5,
- thermalization models $\Longleftrightarrow$ black hole formation models.

The most popular black hole formation models are

- colliding shock waves;
- collapse of stars.

The first model is suitable for the holographic description of heavy ion collisions, and the area of the trapped surface that occurs during the collision of shock waves is associated with the total multiplicity of particles formed in HIC [3, 23, 24, 26].

3. Total multiplicity produced in heavy ions collision

Dependence of the total multiplicity produced in heavy ions collision on energy of the colliding particles has been obtained in the ALICE experiment at LHC, see Fig.2. Note that the bulk of the particles are born immediately after the collision of heavy ions. The result of the ALICE experiment is [22]

$$\mathcal{M} \sim s_{NN}^{0.155}. \tag{1}$$

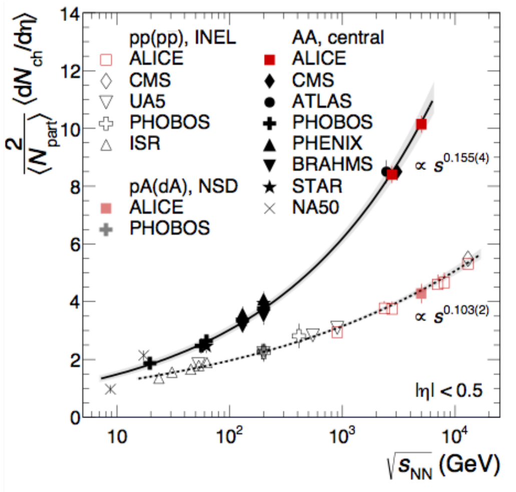

Figure 2: Dependence of the charged-particle multiplicity density at midrapidity in Pb-Pb collisions. Plot from [22]

- The Landau macroscopic theory of high-energy collisions gives

$$\mathcal{M}_{LL} \sim s^{0.25}. \tag{2}$$

- Holographic approach:
  – the simplest model (collision of shock waves) gives [23–27]

$$\mathcal{M}_{AdS} \sim s^{0.33}, \tag{3}$$

  – anisotropic Lifshitz type background with exponent ν [3]

$$\mathcal{M}_{\nu} \quad \sim \quad s^{\frac{1}{2+\nu}}, \tag{4}$$

and for $\nu = 4.45$ we get (1).

4. Holographic model of an anisotropic plasma in a magnetic field at a nonzero chemical potential

4.1. *Action and metric.* A typical action of HQCD model is

$$\int d^5x \sqrt{-g}\left[R - \frac{f_1(\phi)}{4}\,F^2_{(1)} - \frac{f_2(\phi)}{4}\,F^2_{(2)} - \frac{f_B(\phi)}{4}\,F^2_{(B)} - \frac{1}{2}\,\partial_\mu\phi\partial^\mu\phi - V(\phi)\right] \tag{5}$$

with f_1 related to the chemical potential, f_2 to anisotropy, f_B to magnetic field, see [7,13,14,17] for details.

The metric and matter that solve the equations of motion following from action (5) are supposed to be in the special form. The metric is

$$ds^2 = \frac{b(z)}{z^2}\left[-g(z)\,dt^2 + dx^2 + z^{2-\frac{2}{\nu}}dy_1^2 + e^{c_B z^2} z^{2-\frac{2}{\nu}}dy_2^2 + \frac{dz^2}{g(z)}\right]. \tag{6}$$

The 5-coordinate z plays the role of the energy scale. The Maxwell fields are $A^{(1)} = A_t(z)\delta^0_\mu$, $F^{(2)}_{y_1 y_2} = q$, $F^{(B)}_{xy_1} = q_B$ and the scalar field depends only on z. In [17] it has been shown that fixing $b(z)$ and $f_1(\phi)$ one can find f_2, f_B, $\phi(z)$, $V(\phi)$ and $g(z)$.
The overall factor $b(z)$ plays essential role in the properties of the model. It is different for holographic models that correspond to light and heavy quarks, see [7, 13, 14, 17].

4.2. *Phase transition confinement/deconfinement.* One of the goals of the holographic QCD is to describe QCD phase diagram. General requirements on the phase diagram:

- reproduce the QCD results from perturbation theory at short distances,
- reproduce Lattice QCD results at large distances (~ 1 fm) and **small** μ_B.

According to lattice data the phase structure essentially dependents on mass of quarks, see Fig.3.

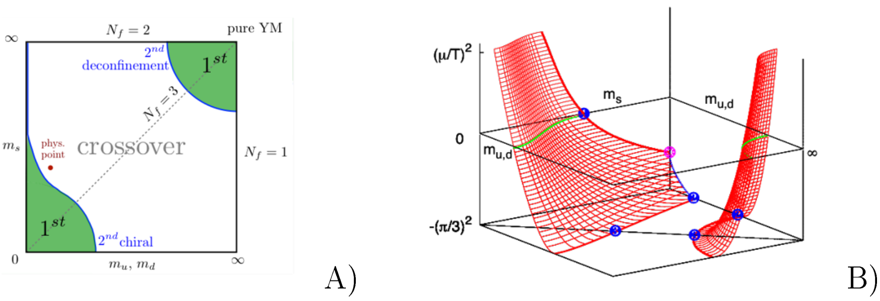

Figure 3: Lattice QCD phase diagrams. A) Columbia plot (plot from [28]). Plot with the imaginary chemical potential (from [29])

The schematic pictures of the structure of phase diagrams for light and heavy quark are presented in Fig.4. For realistic quark mass the expected QCD phase diagrams are presented in Fig.5. General features of these diagrams are similar to the phase diagram for light quark diagram presented in Fig.4.

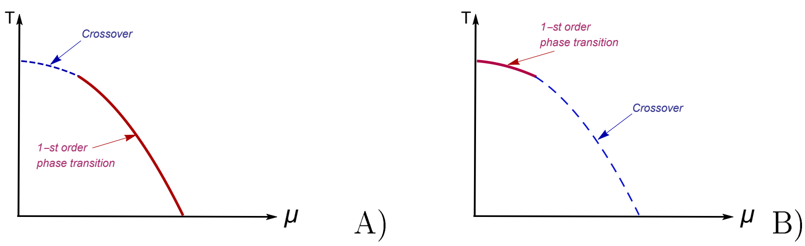

Figure 4: The schematic picture of the phase diagrams structure for light (A) and heavy (B) quarks.

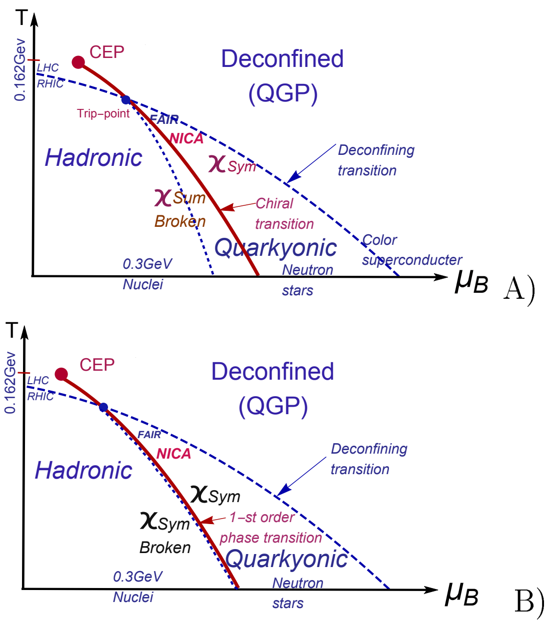

Figure 5: The expected QCD phase diagrams for realistic quark masses (A) and for light quarks (B).

4.3. *Comparison of the 1st order phase transition for light and heavy quarks.* In this section we describe the results obtained in [13]. As it is explained in details there, see also [15], the appearance of the first order phase transition is related to the multivalued dependence of the Hawking temperature on the horizon radius for the metric in the form (6). From Fig.**??** we

$B = 0$ $\quad$ $B \neq 0$

Figure 6: Phase transitions of the 1st order in isotropic (green lines, $\nu = 1$) and anisotropic (blue lines, $\nu = 4.5$) models for light quark models for zero and not zero magnetic fields

see that

- for light quarks, $B = 0$, the onset of the 1st order PTs moves towards $\mu = 0$ as ν increases;
- for heavy quarks, $B = 0$, the 1st order PT line becomes longer with increasing ν;
- as c_B increases (strong magnetic field) phase transition line lengths decrease.

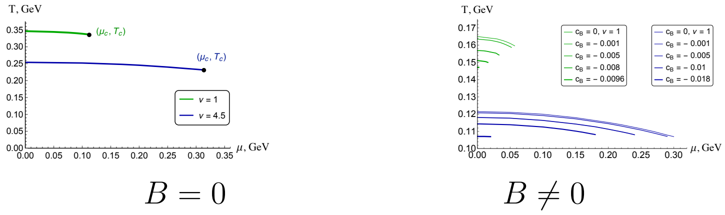

Figure 7: Phase transitions of the 1st order in isotropic (green lines, $\nu = 1$) and anisotropic (blue lines, $\nu = 4.5$) models for heavy quark models for zero and not zero magnetic fields

4.4. *Quarkyonic phase.* Quarkyonic phase appears in the holographic model corresponding to light quarks. In this case the line of the appearence of quarkyonic phase coincides with the chiral symmetry breaking phase, as it is shown in Fig.5. B. We expect that for more realistic holographical model, these two line are separated, as shown Fig.5. A.

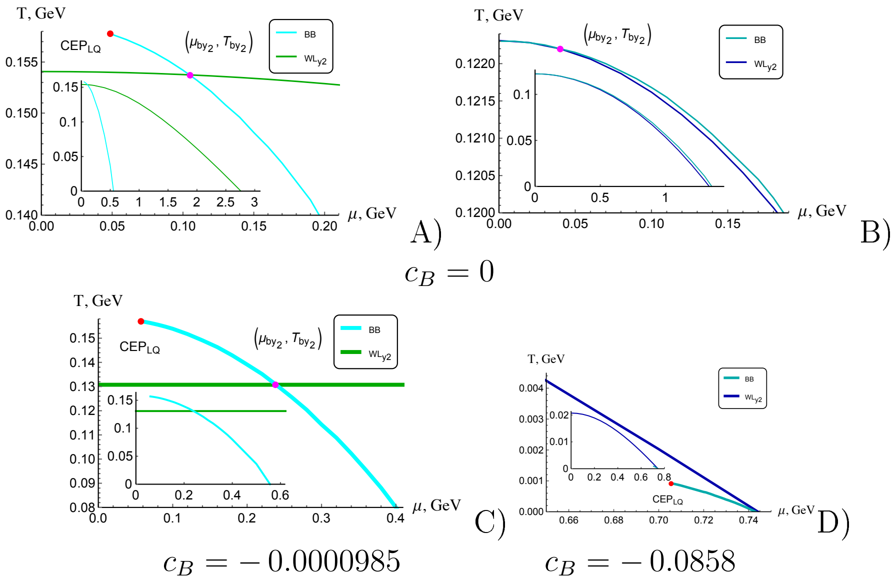

Figure 8: Quarkyonic phase appears during isotropization at large μ for zero magnetic field (A) and B)) and for non-zero magnetic field (C) and D)); $\nu = 1$ for A) and C) and $\nu = 4.5$ for B) and D)

In Fig.8 we show two types of the phase transition lines: the first order transition lines (cyan on A and C, and dark cyan on B and D) associated with background transitions related with instability of small black brane and the second order transition lines (green on A and C, and dark blue B and D) associated with confinement/ deconfinement transition line. These plots are based on detail treatments of holographic time-like Wilson loops in anizotropic modes. These investigations have been performed in our papers [5, 7, 9, 13, 14] and haven't been discussed here.

4.5. *Properties of an anisotropic plasma in a magnetic field at a nonzero chemical potential.* Having a metric that provides a holographic description of the quark-gluon plasma, one can calculate various physical quantities in different phases and find their behavior near the phase transition lines. Of greatest interest are quantities that can be directly measured in collisions of heavy ions. They are

- energy losses – in the holographic approach related with tension of the spatial Wilson loop, see detail calculations for model (5) in [10, 12] ;
- jets quenching – in the holographic approach associated with light-like Wilson loops, for their evaluations for a simplified version of action (5) see [6];
- photon emission rate and electrical conductivity related via

$$d\Gamma \sim \mathrm{Im}\left[\mathrm{tr}\left(\eta_{\mu\nu}G_R^{\mu\nu}\right)\right]_{k^0=|\mathbf{k}|}, \qquad \sigma^{\mu\nu} = -\frac{G_R^{\mu\nu}}{iw}, \tag{7}$$

  for model (5) they have been calculated in [16, 18];
- the entropy of entanglement and the number of particles produced in the chosen volume were estimated in [8, 11].

5. Conclusion

In this talk we have guided that using the holographic model (5), (6) and taking anisotropy into account

- we have reproduced the experimental dependence of particle multiplicity on energy given by (1);
- we found that HQCD, which takes into account anisotropy, has a richer structure of the phase diagram compared to the isotropic model; the phase structure essentially depends on the quark masses, and the quark masses are taken into account by the holographic model itself; i) due to anisotropy one has a smearing of the confinement/deconfinement phase transition,

  ii) the effect of the inverse magnetic catalysis takes place, namely the critical T decreases with increasing of B,

  iii) for light quarks model quarkyonic phase appears during isotropization and is absent for a large value of the anisotropy parameter;
- we also have found dependence of electrical conductivity on

  – anisotropy and quark masses: σ^{11} has weak, σ^{22}, σ^{33} have essential dependencies on anizotropy,Aref'eva I. Ya.

  – magnetic field reduces anisotropy smearing.

References

1. *Aref'eva I. Ya.* Holographic approach to quark–gluon plasma in heavy ion collisions // Phys. Usp. 2014, V. 57, P. 527-555

2. *Aref'eva I. Ya.*, Formation time of quark-gluon plasma in heavy-ion collisions in the holographic shock wave model Teor. Mat. Fiz. **184** (2015) 398-417

3. *Aref'eva I., Golubtsova A.*, Shock waves in Lifshitz-like spacetimes // JHEP 2015 V. 04. P.011

4. *Aref'eva I., Golubtsova A. and Gourgoulhon E.*, Analytic black branes in Lifshitz-like backgrounds and thermalization // JHEP 2016. V.09. 142

5. *Aref'eva I. Ya.* Holography for Heavy Ions Collisions at LHC and NICA // EPJ Web Conf. 2017. V.164, P. 01014

6. *Ageev D., Aref'eva I. , Golubtsova A. and Gourgoulhon E.* Thermalization of holographic Wilson loops in spacetimes with spatial anisotropy // Nucl. Phys. B 2018. V.931. P.506-536

7. *Aref'eva I. and Rannu K*, Holographic Anisotropic Background with Confinement-Deconfinement Phase Transition // JHEP. 2018. V. 05. P. 206

8. *Aref'eva I. Ya.*, Holographic Entanglement Entropy for Heavy-Ion Collisions // Phys. Part. Nuclei Lett. 2019. V.16. P. 486–492

9. *Aref'eva I. , Patrushev A. , Slepov P.* Orientation Dependence of Confinement-Deconfinement Phase Transition in Anisotropic Media // Phys. Lett.B. 2019. V. 792. P. 470

10. *Aref'eva I.* Holography for Nonperturbative Study of QFT // Phys. Part. Nucl. 2020, V.51. no.4. P. 489-496

11. *Aref'eva I. , Patrushev A. , Slepov P.* Holographic Entanglement Entropy in Anisotropic Background with Confinement-Deconfinement Phase Transition // JHEP 2020. V. 07. P. 043

12. *Aref'eva I. Ya., Rannu K. A. and Slepov P. S.* Spatial Wilson loops in a fully anisotropic model // Teor. Mat. Fiz. 2021. V.206. P. 400-409

13. *Aref'eva I. Ya., Rannu K. A. and Slepov P. S.* Holographic Anisotropic Model for Light Quarks with Confinement-Deconfinement Phase Transition // JHEP 2021 V. 06. P. 90

14. *Aref'eva I. Ya., Rannu K. A. and Slepov P. S.* Holographic Anisotropic Model for Heavy Quarks in Anisotropic Hot Dense QGP with External Magnetic Field // JHEP. 2021. V.07. P.161

15. *Aref'eva I. Ya.* Theoretical Studies of the Formation and Properties of Quark-Gluon Matter under Conditions of High Baryon Densities Attainable at the NICA Experimental Complex // Phys. Part. Nucl. 2021. V. 52. P. 512-521

16. *Aref'eva I. Ya., Ermakov K. and Slepov P. S.* Direct photons emission rate and electric conductivity in twice anisotropic QGP holographic model with first-order phase transition // EPJ C. 2022. V.82. P.85

17. *Aref'eva I. Ya., Rannu K. A. and Slepov P. S.* Anisotropic solution of the holographic model of light quarks with an external magnetic field // Theor. Math. Phys. 2022. V. 210. P. 363-367

18. *Aref'eva I. Ya., Ermakov K., Rannu K. A. and Slepov P. S.* Holographic model for light quarks in anisotropic hot dense QGP with external magnetic field // Eur. Phys. J. C 2023. V.83. P. 79

19. *Maldacena J. M.* The Large N limit of superconformal field theories and supergravity// Adv. Theor. Math. Phys. 1998. V.2. P.231-252

20. *Casalderrey-Solana J., Liu H., Mateos D., Rajagopal K. and Wiedemann U. A.* Gauge/String Duality, Hot QCD and Heavy Ion Collisions // 2014 Cambridge University Press

21. *DeWolfe O., Gubser S. S., Rosen C. and Teaney D* Heavy ions and string theory // Prog. Part. Nucl. Phys. 2014. V.75. P.86

22. *Adam J. et al.* [ALICE Collab.] Centrality dependence of the charged-particle multiplicity density at midrapidity in Pb-Pb collisions at $\sqrt{s_{NN}} = 5.02$ TeV. Phys.// Rev. Lett. 2016. V.116, P. 222302

23. *Gubser S. S. , Pufu S. S. and Yarom A.* Entropy production in collisions of gravitational shock waves and of heavy ions // Phys. Rev.D. 2008. V.78. P. 066014

24. *Alvarez-Gaume L. , Gomez C. , Sabio Vera A., Tavanfar A. and Vazquez-Mozo M. A.* Critical formation of trapped surfaces in the collision of gravitational shock waves // JHEP. 2009 V. 02. P. 009

25. *Aref'eva I. Ya., Bagrov A. A.* Formation of trapped surfaces in the collision of nonexpanding gravitational shock waves in an AdS4 spacetime // Theor. Math. Phys. 2010. V. 161. P.1643

26. *Kiritsis E. and Taliotis A.* Multiplicities from black-hole formation in heavy-ion collisions // JHEP. 2012. V. 04. P. 065

27. *Ageev D. S. and Aref'eva I. Ya.* Holographic thermalization in quark confining background// J. Exp. Theor. Phys. 2015. V.120. P. 436-443

28. *Brown F. R. et al.* On the existence of a phase transition for QCD with three light quarks // Phys.Rev.Lett. 1990. V.65. P.2491.

29. *Philipsen O, and Pinke C.* The $N_f = 2$ QCD chiral phase transition with Wilson fermions at zero and imaginary chemical potential // Phys. Rev. D 2016. V.93. P. 114507